Vacuum-ultraviolet spectroscopy and energy spectrum of rare-earth molybdates which are improper ferroelectrics

A. M. Mamedov

S. M. Kirov Azerbaidzhan State University, Baku
(Submitted 9 October 1984; resubmitted 11 June 1985)
Zh. Eksp. Teor. Fiz. **90**, 526–536 (February 1986)

The methods of vacuum-ultraviolet spectroscopy were used to study the optical properties of rare-earth molybdates in the photon energy range $E = 1.0$–35.0 eV at temperatures $T = 10$–600 K. The results were used to calculate the optical functions of these compounds. A study of the influence of temperature revealed anomalies (at temperatures in the region of the phase transition) in the spectrum of the characteristic energy losses in gadolinium molybdate. A scheme of energy transitions in $RE_2(MoO_4)_3$ compounds was constructed on the basis of the results obtained and the dominant role of the MoO_4 tetrahedra in the formation of the energy band structure of these crystals was demonstrated.

INTRODUCTION

There have been many investigations of the electron structure of complex compounds of d-transition metals.[1,2] One of the most important groups among these compounds is a family of rare-earth molybdates which are oxygen-tetrahedral ferroelectrics.

The ferroelectricity of rare-earth molybdates $RE_2(MoO_4)_3$ (RE = Gd, Dy, Tb, Eu, and Sm) was first discovered in the temperature range $420\,K \leqslant T_c \leqslant 460$ K and investigated by Borchard and Bierstedt.[3] These crystals have a number of interesting physical properties and have been attracting the attention of investigators for a long time.[4] Earlier studies of these crystals[5,6] have shown that $RE_2(MoO_4)_3$ are suitable media for the emission of stimulated radiation, i.e., they can be used as laser materials.[7] However, the interest in these compounds goes well beyond their applications. The presence in $RE_2(MoO_4)_3$ of three independent groups of MoO_4 tetrahedra with different MO-O bonds and the relative displacements of the RE^{3+} ions and the MoO_4 sublattices as a result of a phase transition alter many macroscopic and microscopic parameters of these compounds.[8,9] The question of the nature of the ferroelectric state of these oxides is closely related to the electron interactions in them.[9] It would be of interest to study the electron structure and the nature of chemical bonds in $RE_2(MoO_4)_3$, as well as the role of the MoO_4 tetrahedra in the formation of the energy spectrum of electrons.

We used the methods of ultraviolet and vacuum-ultraviolet spectroscopy to investigate for the first time the electron structure of isostructural complex compounds $RE_2(MoO_4)_3$ of d-transition elements in the photon energy range $E = 1.0$–35.0 eV at temperatures $T = 10$–600 K, which included the phase transition region.

EXPERIMENTS

Our $RE_2(MoO_4)_3$ crystals were grown by the Czochralski method and had phase transition temperatures $420\,K \leqslant T_c \leqslant 460$ K deduced from dielectric measurements. The samples of $RE_2(MoO_4)_3$ used in determination of the reflection (R) and transmission spectra were cut from boules and had dimensions of $6 \times 6 \times d$ mm. The thickness d was varied within the range 100–$1500\,\mu$. Crystals were subjected first to mechanical grinding and polishing, and this was followed by annealing in an inert medium in order to relieve the elastic stresses. Immediately before measurements they were subjected to ionic cleaning in ultrahigh vacuum. All the measurements were carried out on mirror-smooth polished faces of Z-cut crystals of $RE_2(MoO_4)_3$ reduced to the single-domain state.

Measurements of the optical properties of $RE_2(MoO_4)_3$ were made using apparatus described in detail in Refs. 10 and 11. The sources of polarized light in the form of synchrotron radiation were SPEAR and TANTALUS storage rings in the USA. The apparatus was modernized and improved so as to carry out spectroscopic measurements in a wide range of temperatures.

REFLECTION AND ABSORPTION SPECTRA

The normal reflection spectra of $RE_2(MoO_4)_3$ crystals determined in the photon energy range $E = 3.0$–35.0 eV are shown in Fig. 1. It is clear from this figure that the spectra of R of all the investigated $RE_2(MoO_4)_3$ compounds have a structure concentrated in two wide bands at $E = 3.0$–16.0 eV ($T = 300$ K) where the reflectivity is $\approx 30\%$. The spectra of R are similar for the various $RE_2(MoO_4)_3$ compounds.

An increase in the energy of the incident photons results in a rapid fall of the reflectivity and there is no clear structure in the spectra of R at energies above 16 eV, which corresponds to failure of the sum rule and excitation of plasma oscillations in the valence band. The absence of singularities in the spectra of R of $RE_2(MoO_4)_3$ at photon energies above 16 eV shows that the valence and conduction bands are separated by large gaps from the other energy bands or that transitions from deeper levels to the conduction band are forbidden by the selection rules.

The first (A) band in the R spectra of $RE_2(MoO_4)_3$ is located at $E \approx 4.5$ eV and has singularities on the low- and

 0038-5646/86/020305-07$04.00

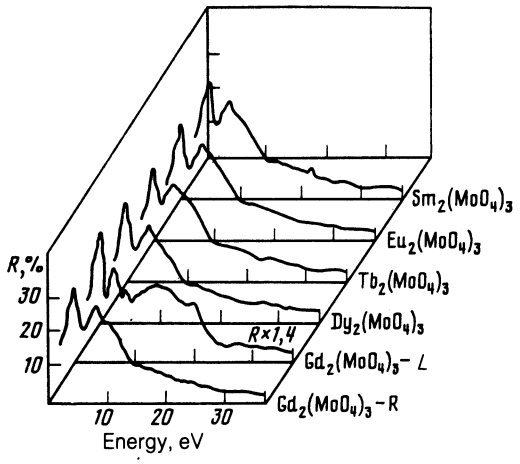

FIG. 1. Reflection spectra of rare-earth molybdates recorded at different temperatures T: 300 K (room temperature R); 15 K (low temperature, denoted by L).

high-energy sides (Table I). The band A has a small half-width and a large oscillator strength. The second (B) band in the spectra of R is located at $E \approx 8.3$ eV and has singularities on the high-energy side (Table I). The band B has a large half-width and a small (compared with the band A) oscillator strength. Cooling complicates the spectra of R, causes splitting of some of the peaks, and gives rise to new singularities. All this is accompanied by a reduction in the reflectivity of single crystals. By way of example, Fig. 1 shows the spectrum of gadolinium molybdate (GMO) at $T = 15$ K. We can see that the maximum of the band A shifts toward higher photon energies, and the temperature coefficient dE_R/dT describing this shift is $\approx -1\times10^{-3}$ eV/K. The value of dE_R/dT is of the same order of magnitude for the other investigated molybdates. The band B splits into three weaker bands with maxima at $E_1 = 7.01$, $E_2 = 9.05$, and $E_3 = 13.80$ eV. A further increase in the energy of the incident photons increases the reflectivity. In the range $E = 18$–25 eV there is a band with a maximum at $E = 19.68$ eV and low-intensity peaks in the high-energy wing of this band. The profile of this band in the spectrum of GMO is characteristic of transitions from deep-lying f energy bands.[12] The major difference between the low-temperature spectrum of R ($T = 15$ K) of GMO and the spectrum of R at room temperature can be explained as follows. A strong temperature dependence of elastic deformation is characteristic of GMO: this results in considerable displacements of the Mo and Gd ions in a unit cell and it alters also the Mo-O bonds.[5,8] Therefore, we may assume that strong cooling of a crystal splits the valence band formed by the $2p$ electrons of oxygen and results in diffuse broadening of the f states of the rare earth.

We also investigated in detail the transmission spectra of single-domain GMO crystals using polarized light of photon energy $E = 2.5$–4.5 eV. These measurements were carried out in a wide temperature range ($T = 15$–600 K). The recorded transmission spectra and the R spectra determined earlier were used to calculate the absorption coefficient α by the usual method.[13] The results of our determination of the photon-energy dependence of α of single-domain GMO samples are presented in Fig. 2 for two polarizations of light. The dependence of α on E is plotted on a semilogarithmic scale at three temperatures T: 80, 330, and 480 K. We can see from this figure that in the case of both polarizations of light the absorption coefficient in the range $\alpha = 10$–10^3 cm^{-1} depends on the photon energy in accordance with the law

$$\alpha = \alpha_0 \exp[S(E-E_0)], \qquad (1)$$

where α_0 and E_0 are the characteristic constants of a given substance, and S is the slope of the absorption edge. These GMO single crystals exhibited an absorption anisotropy. The absorption edge obtained in the $\mathbf{E}\|\mathbf{c}$ case is shifted toward higher energies. The difference between the energy po-

TABLE I. Energy positions (eV) of principal singularities of reflectivity (R) of oxygen-tetrahedral-ferroelectrics at photon energies 3.0–17.0 eV.

Band designation	Singularity	T=15 K			T=300 K		
		GMO	GMO	DMO	TMO	EMO	SMO
	A_1	3.16	–	–	–	–	–
	A_2	3.62	3,68	3.45	3.35	3.70	3.40
	A_3	4,07	–	–	–	–	–
A	A_4	4.30	–	–	–	–	–
	A_5	5.20	4.54	4.40	4.37	4.60	4.60
	A_6	5.65	–	–	–	–	–
	A_7	6,00	5.29	5.52	5.30	5,52	–
	A_8	6.45	–	–	–	–	–
	B_1	–	–	7.13	6.70	6.67	7.00
	B_2	7.01	7,59	7,82	–	7,36	–
	B_3	7.41	–	–	–	–	–
	B_4	–	8.54	8.30	8.20	8,30	8.40
	B_5	8.60	–	8,62	–	–	8,74
	B_6	–	–	8.97	9.25	8.95	–
B	B_7	9,05	9.60	–	–	9.65	9.45
	B_8	9.95	10.35	10.12	10.35	10.81	10.10
	B_9	10,85	11,73	–	–	–	–
	B_{10}	12,00	12.65	12.20	12.90	12,00	12.65
	B_{11}	–	13.10	–	–	–	–
	B_{12}	13.80	13,80	–	–	–	–
	B_{13}	15,16	16,00	–	16.30	–	15.90
	B_{14}	–	17.25	17.00	–	17,00	17.50

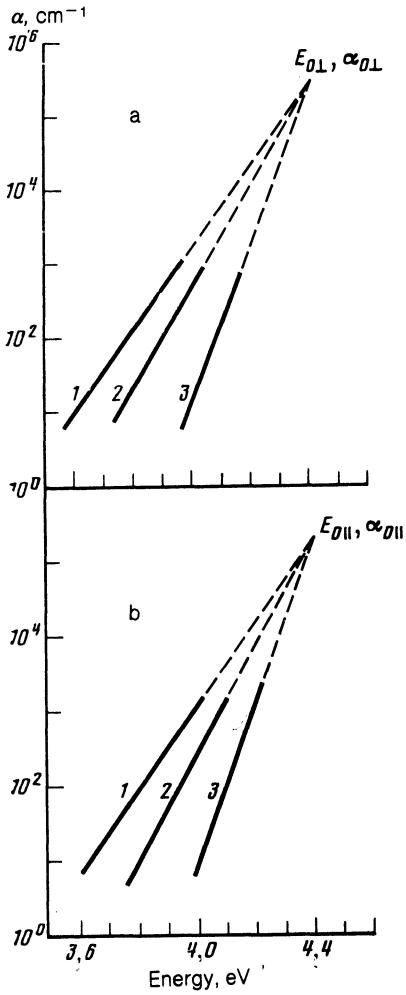

FIG. 2. Dependences of the absorption coefficient α on the energy of photons incident on gadolinium molybdate at temperatures 480 K (1), 330 K (2), and 80 K (3) in the two cases $E \perp c$ (*a*) and $E \parallel c$ (*b*).

sitions of the absorption edge obtained for the two orientations of the plane of polarization of light amounts to 50 meV at $\alpha = 2 \times 10^2$ cm^{-1}. An analysis of the spectral dependence of α shows that the slope of the optical absorption edge is almost the same for both polarizations of light and at room temperature it amounts to a value of the order of 16 eV^{-1}.

An investigation of the temperature dependence of α showed that the photon energy dependence of α obeys an exponential law throughout the investigated temperature range. The slope of the absorption edge depends strongly on temperature: the value of S^{-1} is directly proportional to temperature (Fig. 3). It is also clear from Fig. 3 that the spectral dependence of α both above the phase transition point (paraelectric phase) and below this point (ferroelectric phase) is exponential, i.e., the nature of the optical transitions is not altered by the phase transition.

The average temperature shift of the absorption edge dE_g/dT calculated from the temperature dependence of the energy position of α at $\alpha = 2 \times 10^2$ cm^{-1} amounts to $dE_g/dT = -1.1 \times 10^{-3}$ eV/K in the ferroelectric phase and $dE_g/dT = -3 \times 10^{-4}$ eV/K in the paraelectric phase.

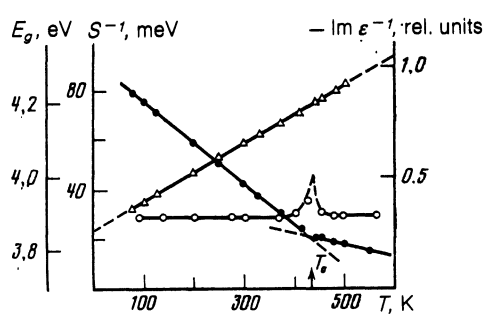

FIG. 3. Temperature dependences of the band gap E_g (●), slope of the absorption edge S (△), and characteristic energy loss function $-\operatorname{Im} \varepsilon^{-1}$ (○) of gadolinium molybdate; $\alpha = 200$ cm^{-1}.

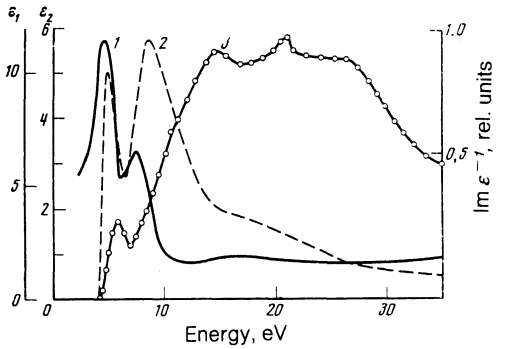

FIG. 4. Spectra of the ε_1 (curve 1) and imaginary ε_2 (curve 2) parts of the permittivity (ε), and of the characteristic energy loss function $-\operatorname{Im} \varepsilon^{-1}$ (curve 3) of gadolinium molybdate at $T = 300$ K.

DISCUSSION OF RESULTS

Kramers-Kronig relationship and optical functions of GMO

The experimental data were analyzed and the optical functions were obtained using the Kramers-Kronig difference method.[14] The phase of the reflected wave and the optical constants (refractive index and extinction coefficient) made it possible to determine the spectral dependences (Figs. 4 and 5) of the real ε_1 and imaginary ε_2 parts of the permittivity $\varepsilon = \varepsilon_1 - i\varepsilon_2$, of the function representing the characteristic energy losses $-\operatorname{Im} \varepsilon^{-1}$, of the effective per-

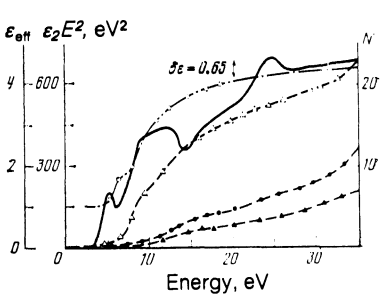

FIG. 5. Energy dependences of the quantity $\varepsilon_2 E^2$ proportional to the combined interband density of states (continuous curve), of ε_{eff} representing the effective optical permittivity (○), and of the effective numbers of the valence electrons governing the intensities of optical transitions (N_{eff}, △) and the appearance of plasma oscillations in the bulk (N_p, ▲) and on the surface (N_s, ●) of a $Gd_2(MoO_4)_3$ crystal.

mittivity ε_{eff}, and of the quantity $\varepsilon_2 E^2$ proportional to the combined interband density of states found by us from the sum rule[15] for the functions $\varepsilon_2 E$; $-\operatorname{Im}\varepsilon^{-1} E$ and $-\operatorname{Im}(\varepsilon+1)^{-1} E$ are the effective numbers of the valence electrons which govern respectively the intensities of optical transitions (N_{eff}) and the appearance of plasma oscillations in the bulk (N_p) and on the surface (N_s) of GMO single crystals at $T = 300$ K. Unfortunately, the absence of data on the behavior of the optical constants in the long-wavelength parts of the spectra of the remaining $RE_2(MoO_4)_3$ compounds prevented us from calculating their optical functions. However, we shall assume that the similarity of the spectra of R of all the investigated $RE_2(MoO_4)_3$ compounds justifies extension of the results obtained for GMO to all other $RE_2(MoO_4)_3$. The spectra of R provide a reasonable opportunity for identification of the main interband transitions on the basis of these functions. However, the most important optical function representing the energy spectrum of electrons is ε_2.

It is clear from Fig. 4 that the spectrum of ε_2 is complex and has a structure concentrated in the photon energy range $E = 3.0$–14.0 eV.

The main structure element in all our crystals is the MoO_4 tetrahedron. The presence of the MoO_4 tetrahedra in the lattice of GMO, the similarity of the optical spectra of GMO to those of the other tetraoxyanions of molybdenum demonstrate an important role of the MoO_4 tetrahedra in the formation of the energy spectrum of GMO and other $RE_2(MoO_4)_3$ compounds. This means that the MoO_4 tetrahedra determine the lower edge of the conduction band and the upper edge of the valence band, and the conduction band is split into two subbands separated by ≈ 4 eV. Such splitting is typical of the electron states of the d-transition metals subjected to a crystal field. The spectra of ε_1 and ε_2 are in good agreement with this conclusion.

At photon energies in excess of 10 eV the spectra of R and ε_2 of GMO single crystals exhibit a fall and there is no clear structure in the spectrum of ε_2 at frequencies exceeding the frequency of the transition from the valence to the conduction band. At this frequency we can expect the influence of plasmons in GMO. The spectrum of the characteristic energy loss function $-\operatorname{Im}\varepsilon^{-1}$ of GMO calculated on the basis of the optical measurements is presented in Fig. 4. It is clear from this figure that $-\operatorname{Im}\varepsilon^{-1}$ has a complex spectrum with maxima both at the energies of single-particle excitations as well as at the energies of plasma resonances. It is known that the maxima of $-\operatorname{Im}\varepsilon^{-1}$ correspond to a plasma resonance when ε_1 and ε_2 tend to zero in the region of a peak of $-\operatorname{Im}\varepsilon^{-1}$ and vary linearly at rates $d\varepsilon_1/dE > 0$ and $d\varepsilon_2/dE < 0$ (Ref. 15). Therefore, the first maximum spectrum of the characteristic energy loss function, located at ≈ 6 eV, is most probably associated with interband transitions. At energies in excess of 10 eV the spectrum of the characteristic energy loss function includes a wide band associated with the excitation of the $2p$ valence electrons of oxygen. It is difficult to determine the energy of plasma oscillations E_p from the spectrum of $-\operatorname{Im}\varepsilon^{-1}$. Therefore, we found the correct value of E_p using the familiar sum rule[15]

$$-\frac{2}{\pi}\int E \operatorname{Im}\varepsilon^{-1} dE = E_p^2 . \qquad (2)$$

The energy dependence of $-\operatorname{Im}\varepsilon^{-1}$ (Fig. 4) and Eq. (2), together with the criterion given above, were used to determine E_p for GMO and this gave the value $E_p = 19.7$ eV.

The optical functions of ferroelectrics are very sensitive to the characteristic mechanisms of the appearance of ferroelectricity.[16] This is confirmed by our data on the optical absorption edge of GMO obtained in the present study. It is worth noting the importance of the effect of temperature on the spectra of the characteristic energy loss functions of improper ferroelectrics and identification of possible changes in this function at the phase transition point. Such measurements also make it possible to reveal how the phase transitions affect the energy position of the bottom of the conduction band and of the deep-lying levels of the atomic cores. An analysis of the influence of temperature on the spectra of the characteristic energy loss function of GMO showed that the temperature dependence obtained at a fixed value of the photon energy ($E = 23.0$ eV) revealed[1)] an anomalous increase in the intensity of $-\operatorname{Im}\varepsilon^{-1}$ in the phase transition region (Fig. 3). We can see from this figure that the intensity of $-\operatorname{Im}\varepsilon^{-1}$ rises slowly in the phase transition region and then falls steeply. Unfortunately the complexity of the experiments and the large volume of computations, as well as difficulties encountered in the stabilization of the temperature in the region of T_c prevented us from investigating in detail the anomalous behavior of $-\operatorname{Im}\varepsilon^{-1}$ in the phase transition region of GMO. Recent papers[17,18] reported experimental observations of a similar effect in barium titanate and triglycine sulfate crystals[17] and an attempt to use the phenomenological theory of ferroelectricity to account for this anomaly in the temperature dependence of the characteristic energy loss function.[18] The anomalous behavior of this function of GMO single crystals was first described in Ref. 11, but we were unable to account for this effect. However, we could draw one definite conclusion. The effect in question is more complex than assumed in Ref. 18. This is manifested both by the fact that it is exhibited by such a classical material as barium titanate, which has a strong anomaly of the low-frequency permittivity $\varepsilon(0, T)$, and by improper ferroelectrics such as GMO.

Atomic core levels ($4f$ electrons in rare earths)

At photon energies in excess of 20 eV the spectra of rare-earth molybdates exhibit a weak but strongly broadened structure with a low reflectivity, which can not be attributed to $2p \rightarrow 4d$ transitions between O and Mo. We shall therefore attempt to classify the observed transitions on the basis of the experimental data obtained by us earlier in studies of x-ray photoelectron spectra of tetraoxyanions of transition elements and rare earths.[19–21] The most probable optical transitions in this range of photon energies are those between the $4f$ electron states of the rare earth and the vacant d states of Mo (or the O $2s \rightarrow$ Mo $3d$ transitions).

In view of the above comments, we shall use the data on the energy levels of the atomic cores ($2s$ levels of O and $4f$ levels of RE) and the positions of the maxima of the density

TABLE II. Energy positions (eV) of principal singularities of reflectivity (R) of oxygen-tetrahedral ferroelectrics at photon energies 17.0–35.0 eV.

Band designation	Singularity	$T=15$ K			$T=300$ K		
		GMO	GMO	DMO	TMO	EMO	SMO
C	C_1	18.10	18.78	–	–	18.40	–
	C_2	–	19.70	–	–	–	–
	C_3	19.68	20.58	20.36	–	–	20.00
	C_4	–	21.72	21.94	–	21.75	21.49
	C_5	–	22.62	–	–	–	–
	C_6	23.07	23.75	–	23.75	23.07	23.90
	C_7	24.43	–	–	–	–	–
	C_8	–	26.47	27.15	–	26.70	26.70
	C_9	26.70	–	–	–	–	–
	C_{10}	–	–	29.41	28.28	29.85	–
	C_{11}	30.31	31.90	31.00	–	–	–
	C_{12}	32.80	34.61	–	33.93	33.42	34.00

of the valence states of the $2p$ levels of O from the x-ray photoelectron spectra reported in Refs. 1, 19, and 20. Then, in a simple atomic analysis the bands observed in the energy range $E = 20$–35 eV may be attributed to transitions from the $4f$ states of rare earths and the $2s$ states of O to the vacant states of Mo forming the conduction band. A comparison of our data with the results deduced from x-ray photoelectron spectra made it possible to attribute the transitions to the d states of Mo (in the photon energy $E = 20$–35 eV) to the atomic core levels: $4f$ RE$\rightarrow 3d$ Mo (for example, peaks C_8 and C_{12}), as shown in Table II.

The R spectra of samarium (SMO), terbium (TMO) and dysprosium (DMO) molybdates show that in the region of 25–35 eV there are no maxima associated with the $4f$ states of the rare earths, but only weak singularities in the optical spectra of these compounds, whereas in the case of GMO and europium molybdates (EMO) there are maxima due to the $4f$ states of the rare earth.

Sum rule and effective number of valence electrons per MoO_4 tetrahedron

The known sum rules[15] can be used to determine some quantitative parameters, particularly the effective number of the valence electrons N_{eff} (and also the values of N_p and N_s) as well as the optical permittivity ε_{eff}, which make contributions to the optical constants of a crystal at an energy E_0. We recall that

$$\int_0^{E_0} E\varepsilon_2\, dE = \frac{2\pi^2\hbar^2}{m} N_a e^2 N_{\text{eff}}, \tag{3}$$

$$\frac{2}{\pi}\int_0^{E_0} E^{-1}\varepsilon_2\, dE = \varepsilon_{\text{eff}}^{-1} \tag{4}$$

(where N_a is the density of atoms in a crystal; e and m are, respectively, the charge and mass of an electron), we shall determine N_{eff} and ε_{eff} from the data obtained by us earlier.

The physical meaning of ε_{eff} is quite clear: ε_{eff} is the effective optical permittivity governed by interband transitions in the energy range from 0 to E_0, i.e., by the polarization of the electron shells. The photon energy dependence of ε_{eff} obtained by us for GMO is a curve (Fig. 5) which can be separated into two regions. The first is characterized by a rapid rise and it extends up to 17 eV. In the second region the value of ε_{eff} rises more smoothly and slowly and tends to saturation at energies 35 eV. This means that the greatest contribution to ε_{eff} is made by transitions corresponding to the bands at 4.5 and 8.3 eV (their contribution amounts to $\approx 85\%$).

The contribution made to the static permittivity $\varepsilon(0)$ by optical transitions at photon energies $E > E_0$ can be determined by comparing the maximum value of ε_{eff} with the square of the refractive index n^2 measured in the transparency range. The difference

$$\delta\varepsilon = n^2 - \varepsilon_{\text{eff}} \neq 0$$

shows the need to allow for the polarizability of deep-lying levels. The difference $\delta\varepsilon = 0.65$ indicates that a large contribution to the static permittivity is made by interband transitions with $E > E_0$ (for example, the transitions involving the $4f$ states of the rare earth).

The value of N_{eff} determined from the sum rule (4) is the effective number of the valence electrons per each atom in a crystal at an energy E_0 (on condition that at this energy E_0 all the possible interband transitions have already taken place). In the case of GMO the number N_{eff} rises almost monotonically on increase in the photon energy (Fig. 5) and shows no tendency to saturation throughout the investigated energy range. Therefore, it is not possible to select some independent criteria for estimating the number of the valence electrons per one unit cell. Bearing in mind that the two conduction subbands are separated from one another and also from higher-lying states in the conduction band, we may postulate a tendency to saturation at energies where the transitions to the corresponding subbands have already taken place ($E = 5.1$, 7.9, 10.0, 14.2 eV). Our values of N_{eff} (calculated using the nominal ion charges) are of the same order of magnitude at these energies as the calculated values (the number of the valence electrons forming the $2p$ band of oxygen is 24).

Application of the sum rules[15] to the calculation of N_p and N_s gave us values which behaved in the same way as N_{eff}, but the corresponding curves were located below N_{eff}. A formal analysis of the relationships used in the calculations of N_{eff}, N_p, and N_s (Ref. 15) shows that integration over the energy range covering all the transitions from the

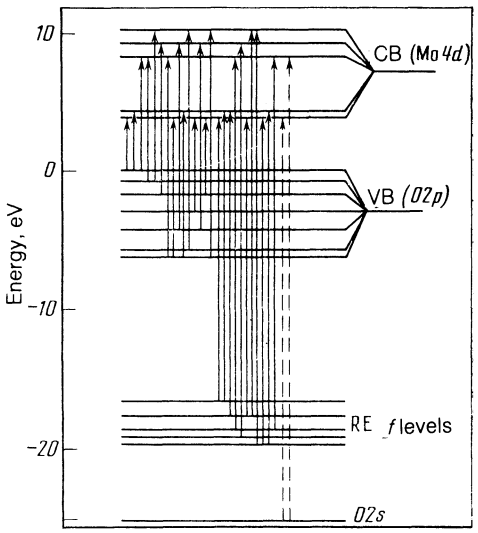

FIG. 6. Interband transitions in $RE_2(MoO_4)_3$ compounds. Here, CB and VB denote the conduction and valence bands, respectively.

valence bands to the conduction band should ensure that N_{eff}, N_p, and N_s converge to the same value, which is equal to the number of the valence electrons. Therefore, the low values of N_p and N_s, compared with N_{eff}, and also the absence of the tendency of N_{eff} to reach saturation at high photon energies indicate that in the energy range $E > 20$ eV we can expect not only transitions from the $2p^6$ band of O^{2-} but also from the $4f$ band of RE, for example, transitions which are orbitally promoted or those involving charge transfer between the RE ions. It also follows that the transitions from the $2p$ and $2s$ bands of O^{2-} and from the $4f$ band of RE can occur even beyond 35 eV. This is confirmed by the fact that the value of $\varepsilon_2 E^2$ at the high-energy edge not only remains large but continues to rise even at the range $E > 30$ eV.

Electron structure of MoO_4 tetrahedron

Studies of the structure of GMO and other $RE_2(MoO_4)_3$ compounds were reported by Keve *et al.*[8] They showed that $RE_2(MoO_4)_3$ consists of three independent groups of the MoO_4 tetrahedra forming consecutive layers along the c axis. The RE^{3+} ions occupy positions close to the centers of REO_7 polyhedra with an average RE-O distance of about 0.233 nm. The average Mo-O distance is approximately 0.175 nm. All this shows that the crystal structure of GMO is very complex and a calculation of the energy band structure of GMO would be a difficult task not yet carried out.

However, as pointed out earlier, the presence of the BO_4 tetrahedra (B = Ti, Mo, Mn, Cr, etc.) in tetraoxyanions of transition metals and the similarity of their optical properties[22] indicate that the BO_4 tetrahedra play the dominant role in the formation of the energy spectrum of tetraoxyanions of transition metals, including those in $RE_2(MoO_4)_3$ compounds. This hypothesis can be tested and the results obtained by us can be interpreted using the theoretical and experimental data on the electron structure of transition metal tetraoxyanions.[1,2,23] We shall assume that this approach is valid in the light of the above discussion.

Several nonempirical calculations of the ground state of tetraoxyanions of the d-transition metals have yielded the following sequence of the valence states: $4t_2$, $5a_1$, $5t_2$, $1e$, $6t_2$, $6a_1$, $1t_1$ (Ref. 23). Calculations carried out by the X_α scattered wave method confirm this scheme.[24] Calculations[25] made for MnO_4^{2-} allowing for the relaxation effect reduce monotonically the energies of the levels of this complex and predict no significant changes in the sequence of the molecular orbitals. They show however that the main changes are in the form of inversion of nonbonding ligand orbitals $1t_1$ and $6a_1$. It is known that the chemical binding in tetraoxyanions is due to the s, p, and d electrons of the metal and the $2p$ electrons of oxygen. In this case the x-ray spectra of the central atom and the ligand should give a full picture of the distribution of their electron densities between the molecular orbitals. In the case of complex tetraoxyanions the d-electron density of the central atom transforms in accordance with the irreducible symmetry representations t_2 and e, whereas the $2p$ electrons of oxygen transform by irreducible representation of the symmetries t_2, e, t_1, and a_1. The relative positions of oxygen and molybdenum[26] suggest that in the case of the $(MoO_4)^{2-}$ tetrahedra the upper filled levels are the molecular orbitals which include the $2p$ electron density of oxygen, whereas the d states of Mo represent the vacant molecular orbitals of this complex. A combined analysis of the theoretical calculations of the electron structure and x-ray spectra of molybdenum tetraoxyanions was made in Ref. 26 and the following sequence of molecular orbitals was suggested: $5t_2$, $1e$, $6t_2$, $1t_1$, $6a_1$. Since GMO contains a fundamental structure element in the form of the MoO_4 tetrahedra, the main features of the energy spectrum calculated for transition-element tetraoxyanions should be retained also in the case of GMO. Naturally, because of the $4f$ wave functions of RE^{3+} and the various types of $4f$-bonds, there should be some changes. This is confirmed also by the optical data; as in the case of transition-metal tetraoxyanions, the two principal optical oscillators corresponding to the photon energies 4.7 and 8.5 eV (Fig. 2) represent transitions from the valence to the conduction band, the latter consisting of two subbands. The presence of other finer structures in the optical spectra of $RE_2(MoO_4)_3$ at photon energies $E = 3.0$–15.0 eV is due to the distortion of the BO_4 tetrahedra, since this causes changes in the symmetry group from T_d to D_{2v}^3 and then to C_{2v}^8.

The results obtained in our analysis thus provide a simple scheme of interband transitions in $RE_2(MoO_4)_3$, shown in Fig. 6, which describes the results obtained.

CONCLUSIONS

Synchrotron radiation was used in a study of the optical properties of improper ferroelectrics in the form of rare-earth molybdates at photon energies 1.0–35.0 eV and their optical functions were calculated. Anomalous behavior of the characteristic energy loss function of gadolinium molybdate was detected and investigated. The results obtained made it possible to construct the energy transition scheme for $RE_2(MoO_4)_3$ crystals and to confirm the dominant role

of the MoO_4 tetrahedra in the formation of the energy band structure of these compounds.

The author regards it as his pleasant duty to thank E. Rowe, D. W. Lynch, F. Ullman, and V. L. Rehn for their help during actual experiments, to the Nebraska State University and to the Ames Laboratory of the Commission on Atomic Energy for subsidizing the experiments, and to G. Smolenskiĭ and V. Bagiev for valuable discussions and comments.

[1)]The anomalous behavior of $-\operatorname{Im}\varepsilon^{-1}(T)$ was observed in the photon energy range $E = 18$–26 eV, i.e., where ε_1 and ε_2 were small and plasmons were observed in GMO.

[1]T. Sasaki and H. Adachi, J. Electron Spectrosc. **19**, 261 (1980).
[2]J. A. Tossell, J. Electron Spectrosc. **8**, 1 (1976).
[3]H. J. Borchard and P. E. Bierstedt, J. Appl. Phys. **38**, 2057 (1967).
[4]S. E. Cummins, Ferroelectrics **1**, 11 (1970).
[5]L. E. Cross, A. Fouskova, and S. E. Cummins, Phys. Rev. Lett. **21**, 812 (1968).
[6]E. Pytte, Solid State Commun. **8**, 2101 (1970).
[7]Kh. S. Bagdasarov, G. A. Bogomolov, A. A. Kaminskiĭ, V. A. Meleshina, T. M. Prokhortseva, and L. A. Shuvalov, Izv. Akad. Nauk SSSR Ser. Fiz. **35**, 1849 (1971).
[8]E. T. Keve, S. C. Abrahams, and J. L. Bernstein, J. Chem. Phys. **54**, 3185 (1971).
[9]A. P. Levanyuk and D. G. Sannikov, Fiz. Tverd. Tela (Leningrad) **12**, 2997 (1970) [Sov. Phys. Solid State **12**, 2418 (1971)]; V. G. Vaks, Vvedenie v mikroskopicheskuyu teoriyu segnetoélektrikov (Introduction to the Microscopic Theory of Ferroelectrics), Nauka, M., 1973, p. 328.
[10]A. M. Mamedov, Zh. Eksp. Teor. Fiz. **83**, 1804 (1982) [Sov. Phys. JETP **56**, 1043 (1982)]; Avtoreferat kand. dissertatsii (Author's Abstract of Thesis for Candidate's Degree), Leningrad, 1975.
[11]A. M. Mamedov and A. H. Zejnally, Proc. Second Japanese-Soviet Symp. on Ferroelectricity, Kyoto, 1980, in: J. Phys. Soc. Jpn. **49**, Suppl. B, 125 (1980).
[12]Yu. V. Knyazer and M. M. Noskov, in: Élektronnaya struktura i fizicheskie svoĭstva redkikh zemel' i aktinidov (Electron Structure and Physical Properties of Rare Earths and Actinides), Ural Scientific Center, Academy of Sciences of the USSR, Sverdlovsk, 1981, p. 3.
[13]Yu. I. Ukhanov, Opticheskie svoĭstva poluprovodnikov (Optical Properties of Semiconductors), Nauka, M., 1977, p. 366.
[14]R. K. Ahrenkiel, J. Opt. Soc. Am. **61**, 1651 (1971).
[15]D. Pines, *Elementary Excitations in Solids*, Benjamin, New York, 1963 (Russ. transl., Mir, M., 1965, p. 382).
[16]V. M. Fridkin, Segnetoélektriki-poluprovodniki, Nauka, M., 1973, p. 408 (Ferroelectric Semiconductors, Consultants Bureau, New York, 1980).
[17]M. T. Lagare and N. Umakantha, Phys. Rev. Lett. **49**, 1431 (1982).
[18]V. L. Ginzburg and A. A. Sobyanin, Fiz. Tverd. Tela (Leningrad) **25**, 2017 (1983) [Sov. Phys. Solid State **25**, 1163 (1983)].
[19]É. A. Kravtsova, Zh. Strukt, Khim. **23**, No. 5, 55 (1982).
[20]Yu. P. Irkhin, V kn.: Élektronnaya struktura i fizicheskie svoĭstva redkikh zemel' i aktinidov (Electron Structure and Physical Properties of Rare Earths and Actinides) Ural Scientific Center, Academy of Sciences of the USSR, Sverdlovsk, 1981, p. 50.
[21]H. Höchst, P. Steiner, G. Reiter, and S. Hüfner, Z. Phys. B **42**, 199 (1981).
[22]R. Grasser, E. Pitt, A. Scharmann, and G. Zimmerer, Phys. Status Solidi B **69**, 359 (1975).
[23]R. D. Brown and W. J. Camber, Inorg. Chim. Acta Rev. **6**, 7 (1972).
[24]V. A. Gubanov, Avtoreferat dokt. dissertatsii (Author's Abstract of Thesis for Candidate's Degree), Sverdlovsk, 1978.
[25]L. N. Mazalov, Zh. Strukt. Khim. **18**, 607 (1977).
[26]R. Kebabcioglu and A. Müller, Chem. Phys. Lett. **8**, 59 (1971).

Translated by A. Tybulewicz